Eur. Phys. J. B **2**, 381–391 (1998)

THE EUROPEAN PHYSICAL JOURNAL B

Cavitation in superfluid helium-4 at low temperature

H. Lambaré[1], P. Roche[1,a], S. Balibar[1], H.J. Maris[2], O.A. Andreeva[3], C. Guthmann[1], K.O. Keshishev[3], and E. Rolley[1]

[1] Laboratoire de Physique Statistique de l'École Normale Supérieure, associé au CNRS et aux Universités Paris 6 et 7, 24 Rue Lhomond 75231, Paris Cedex 05, France
[2] Department of Physics, Brown University, Providence, RI 02912, USA
[3] Academy of Sciences of Russia, Institute for Physical Problems, Kosygin Street 2, Moscow 117334, Russia

Received: 15 November 1997 / Received in final form: 19 December 1997 / Accepted: 22 January 1998

Abstract. We have studied the nucleation of bubbles in pure superfluid helium-4 at temperatures down to 65 mK. We have found that the nucleation is a stochastic process, and that at temperatures below 600 mK the nucleation rate is independent of temperature. These results are consistent with the assumption that the nucleation takes place *via* quantum tunneling.

PACS. 67.20.+k Quantum effects on the structure and dynamics of nongenerate fluids (e.g., normal phase liquid ^{4}He) – 47.55.Bx Cavitation – 64.60.Qb Nucleation

1 Introduction

The liquid-gas transition is a first order phase transition. It follows that there is an energy barrier to overcome for the nucleation of the gas phase, and consequently liquids exist below their saturated vapor pressure P_{sv} for a certain time before nucleation of the gas phase takes place. If special care is taken with purity and container walls, liquids can be stressed down to large negative pressures, *i.e.* far below P_{sv}, before cavitation occurs. A spectacular example is water which has been stressed down to -1000 bars [1]. However, there is an absolute limit known as the "spinodal line" for the metastability of a liquid. This is the spinodal pressure P_{sp}, or spinodal density ρ_{sp}, where the compressibility diverges. Indeed, as one applies an increasing stress to a liquid, one works against the internal forces which are responsible for the liquid cohesion; these cohesive forces decrease with distance so that, as the density decreases, one has to reach a point where the liquid breaks, *i.e.* where the gas phase appears. Since the spinodal pressure depends on temperature, the spinodal lies on a curve in the phase diagram in the (P,T) plane. Spinodal lines exist for all first order phase transitions, and the question "how close can one approach the spinodal line?" is much more general than a problem just related to the stability of a liquid. However, the liquid-gas spinodal and the nucleation of the gas from the liquid is of special interest because the liquid-gas transition is the simplest type of first-order phase transition. In addition, cavitation in liquids is an important practical problem in modern hydraulics, which is still without complete understanding [2].

On the spinodal line, the compressibility is infinite, the sound velocity is zero, there is no energy barrier between the liquid and the gas phase, and the liquid is totally unstable. For pressures slightly positives with respect to the spinodal ($P > P_{sp}$), the energy barrier against nucleation of gas is finite, but at finite temperatures it can be overcome as a result of thermal fluctuations. This process is often referred to as thermal nucleation. Because of this thermal nucleation, the spinodal line can only be approached in experiments performed at very low temperatures. However, for most liquids such experiments are impossible because the liquid solidifies. From this point of view, liquid helium is a very interesting exception. Due to the small mass of a helium atom and to the weakness of attractive forces between atoms, liquid helium is stable down to absolute zero and only freezes above a pressure of $+25$ bars [3] . Furthermore, at 2.17 K a transition takes place to a superfluid quantum state with no viscosity and infinite thermal conductivity. This superfluid liquid can be easily prepared in a very pure state, and has been so well studied and modelled that the spinodal limit at $T = 0$ can be accurately predicted. Sound velocity extrapolations [4], sophisticated density functional calculations [5], as well as Monte Carlo simulations [6] have shown that, at $T = 0$, the spinodal point is close to -9.5 bars. At this pressure, Maris [4] predicts that the spinodal density ρ_{sp} is about 0.095 g cm^{-3}, significantly less than 0.145 g cm^{-3}, the liquid density at $P = 0$ and $T = 0$. It is thus an experimental challenge to determine if superfluid helium at very low temperature can be stressed down to pressures in the vicinity of P_{sp}.

[a] e-mail: proche@physique.ens.fr

It is also expected [7–9] that nucleation of the gas can occur *via* quantum tunneling through the energy barrier: the quantitative prediction [8,9] is that, at a pressure a few tenths of a bar higher than P_{sp}, a macroscopic quantity of liquid helium can tunnel from a metastable state with a reduced homogeneous density to an inhomogeneous state with an essentially empty cavity of the volume of the order of 1000 atoms. Liquid helium thus offers a unique opportunity to approach the spinodal limit as closely as possible, and, in the vicinity of the spinodal, one should observe a spectacular and macroscopic quantum effect. The probability for this "quantum cavitation" was calculated [8,9], and the crossover temperature T^* from quantum to thermal cavitation was estimated to be about 200 mK.

In this paper we describe in detail an experiment which was designed to look for quantum cavitation. It was actually started in our laboratory by Pettersen, and an article describing results at high temperature ($T > 0.8$ K) has already been published [10]. As we shall explain below, our new results are consistent with the prediction of quantum tunneling close to the spinodal limit. We have considered, and ruled out to a reasonable degree of certainty, various possible artefacts which could mimic quantum cavitation.

2 Experiment

The experimental cell is attached to the mixing chamber of a dilution refrigerator. This cell has previously been used for the study of the surface of helium crystals [11]. The cell has four large windows providing optical access in two perpendicular directions. A limiting temperature of 20 mK can be reached as a result of the careful control of thermal radiation. We produce large pressure oscillations in superfluid helium by focusing ultrasonic waves, and we detect cavitation by light scattering, as previously done by Nissen *et al.* [12].

2.1 Acoustic transducer

The sound waves are generated by a hemispherical piezoelectric transducer or "ceramic" [13] with an inner radius r_{tran} of 8 mm and a wall thickness of 2 mm. It resonates in a thickness mode at a frequency close to 1 MHz. At the acoustic focus, the local pressure oscillates by several bars around the static pressure P_{stat} in the cell. This acoustic focus is very close to the center of the hemisphere [14]. Its typical size is half of the wavelength of the acoustic wave, *i.e.* ~ 0.12 mm at this frequency and near $P_{stat} = 0$. The transducer sits on three horizontal wires, with its concave side facing down. Attenuated light from a 10 mW He-Ne laser is focussed onto the acoustic focus and then, after going through the cell, is detected by a photomultiplier. To enable the light to reach and to leave the acoustic focus two small slits have been cut in the lower rim of the transducer. These slits are about 1 mm by 1 mm. They are large enough to pass the light beam, but still sufficiently small that their effect on the acoustic modes of the ceramic is unimportant.

We used pulses of sound with a duration between 30 and 70 μs and a repetition rate in the range 0.1 to 1 Hz. As described in the next section, one of our main observations was that cavitation was stochastic: some sound pulses produce cavitation, some do not. By counting cavitation events, we measure how the cavitation probability depends on the sound amplitude, and repeat this measurement for different static pressures and temperatures. For measurements of the cavitation probability to be of value, it is necessary for the wave amplitude to be constant from one pulse to the next.

2.1.1 The generator

To generate the pulses we used a low level RF generator (Toellner model 7711) followed by a power amplifier. The amplifier was made in our laboratory and used an APEX type PA09 chip. In a push-pull operating mode, this amplifier could deliver an RF pulse of amplitude 70 V, *i.e.* an average power of 50 W in 50 Ω. For an accurate measurement of the cavitation probability, we needed to stabilize the amplitude of the RF pulse applied to the transducer. The power amplifier was enclosed in a box with temperature regulation. The RF pulse was measured by a digital oscilloscope (Tektronix model 2221A) before and after each measurement of the nucleation rate. To improve the base resolution of the oscilloscope (8 bits), the RF pulse waveform was fit to a sine function. This procedure gave a resolution of one part in 10^4 for the amplitude and the frequency. The fluctuation in amplitude from pulse to pulse was of the order of 0.1%, and the long term drift in the amplitude was typically about 0.1% per hour. Since we observed that the cavitation probability goes from 0 to 1 in a voltage interval of about 2% of the cavitation voltage itself, the stability of the electronic system was adequate for the purposes of the experiment.

2.1.2 Resonance frequencies

As a first step towards the analysis of the transducer we measured its electrical impedance as a function of frequency. The measured impedance revealed resonances from a large number of modes. The fundamental thickness mode is at $\omega_0 \approx 1$ MHz, and the lowest frequency breathing mode is at 100 kHz. An isolated resonance of a transducer can be modeled by a capacitance C_0 in parallel with the three elements of a "motional branch", a resistance R, an inductance L and a capacitance C [15]. Thus the impedance is given by the equation

$$\frac{1}{Z} = i\omega C_0 + \frac{1}{R + i(L\omega - 1/\omega C)} \cdot \tag{1}$$

Since ωC_0 is usually small compared to $1/R$, the magnitude of the impedance can be approximated by

$$|Z| = R\left[1 + 4Q_0^2(\omega - \omega_0)^2/\omega_0^2\right]^{1/2}, \tag{2}$$

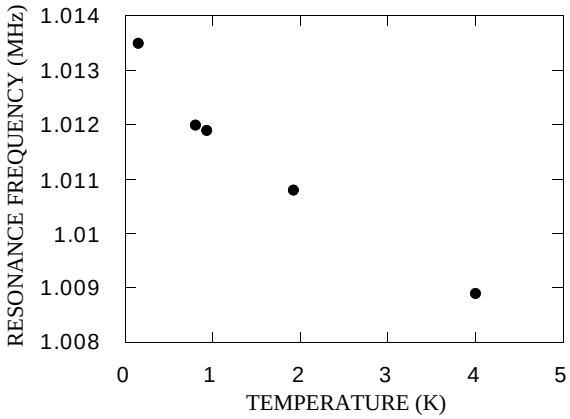

Fig. 1. Resonance frequency of the transducer as a function of temperature.

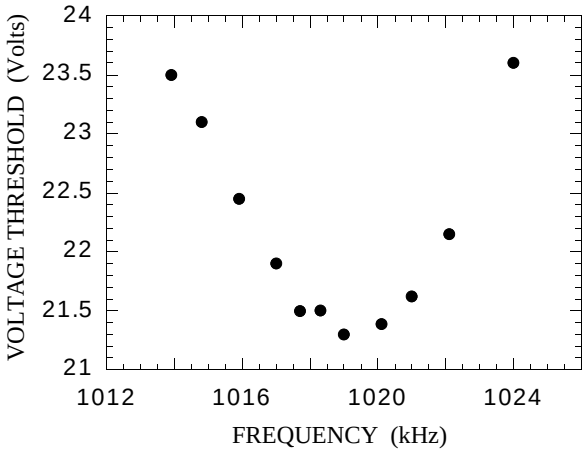

Fig. 2. The cavitation threshold (in Volts applied to the transducer) as a function of frequency. This particular series of measurements was performed with a pulse width of 70 μs, at $P_{stat} = 0.1$ bar and $T_{stat} = 250$ mK.

where $\omega_0 = (LC)^{-1/2}$ is the resonance frequency, and $Q_0 = 1/RC\omega_0$ is the quality factor. We noticed that even at temperatures of a few K, the parameters of the transducer have a significant variation with temperature. The resonance frequency of the transducer ω_0, defined by means of a fit to the measured impedance, was found to vary by about 1.6 kHz per K (see Fig. 1). It was found that there was a small but significant difference between this frequency and the frequency ω_c at which the voltage required to produce cavitation was a minimum. Sample results of measurements of the frequency dependence of the voltage required to produce cavitation are shown in Figure 2. In order to be able to study the variation of the cavitation threshold as a function of T, it was advantageous to choose to work at the frequency ω_c (1.019 MHz) which gives a minimum cavitation threshold V_c for the lowest temperature, rather than at the frequency at which the electrical impedance was a minimum. This choice means that a shift in the resonance frequency of the transducer gives only a second order change in the sound amplitude, rather than a first order effect.

2.1.3 Pulse width

The next problem was the choice of a pulse width τ_p. In the experiments reported here we used much shorter pulses, 30 to 70 μs, than Pettersen *et al.* [10]. Short pulses were used so that the total amount of heat deposited into the cell is reduced, and so that heat dissipated in the transducer cannot reach the acoustic focus in time to affect the nucleation process. While investigating the effect of variation in the pulse length we made the interesting discovery that with sufficiently long pulses multiple cavitation events can be seen. The time interval between two events was about 68 μs. We believe that the explanation of these observations is as follows. When the first cavitation event occurs, a part of the sound pulse is reflected by the cavitation bubble. The reflected sound returns to the transducer after a time r_{tran}/c which is approximately 34 μs. It is then reflected back towards the acoustic focus and arrives there at 68 μs after the first cavitation event. If this reflected acoustic wave arrives in phase with the waves arriving at the same time and coming directly from the transducer surface, there will be a sudden temporary increase in the sound amplitude at the transducer focus. A second cavitation event will then take place. A reflection from this second event can lead to a third event and so on.

2.1.4 Repetition rate

The repetition rate of the acoustic pulses was chosen within the range 0.1 to 1 Hz. Since we usually counted bubbles by watching oscilloscope traces, rather than by an automated method, it was not convenient to use repetition rates larger than 1 Hz. Moreover, for the experiments at the lowest temperatures, we had to be careful with the energy dissipated in the cell. A pulse of amplitude 20 V gave a dissipation rate inside the cell during the pulse of 2 W. Hence, for a pulse duration of 50 μs and a repetition rate of 1 Hz the average power is 100 μW. To make measurements below 100 mK it was therefore necessary to reduce the repetition rate below 1 Hz.

As well as considering the average dissipation it is important to consider what happens to the energy deposited by each single RF pulse. Most of the pulse energy is dissipated in the transducer either by the mechanical dissipation or by dielectric loss. This changes the transducer temperature. The heat capacity of lead zirconate has been measured by Lawless [16]. Based on his results we estimate that for a pulse of amplitude 20 Volts, duration 50 μs and total dissipation 1×10^{-4} J, the temperature of the transducer rises to 3 K. If one half of this energy were immediately released into the 1 cm^3 volume of liquid inside the hemisphere, it would raise the temperature to about 0.4 K. Fortunately, the heat release is delayed by the thermal resistance of the ceramic material and by the Kapitza resistance between the ceramic and the helium. The thermal conductivity κ of lead zirconate between 2 and 4 K is $\approx 6.6 \times 10^{-5} T^2$ W cm^{-1} K^{-1} [16]. Thus the thermal diffusivity of the ceramic at 3 K is 4 cm^2 s^{-1}. The time for heat to diffuse a distance of 1 mm is thus 2500 μs. Since the

thickness of the transducer wall is 2 mm the fraction of the heat which escapes into the helium during the period before the cavitation is observed will be very small. We have performed a detailed calculation of the heat flow in the ceramic, based on the assumption that heat is generated uniformly throughout the thickness. For a drive time of 50 μs we find that the amount of heat which has escaped from the inner surface of the transducer within the first 50 μs is less than 10^{-6} J. If this were distributed uniformly through the liquid inside the hemisphere the temperature would rise to around 180 mK; this rise would not appreciably affect our experimental results. This calculation neglects the effect of the Kapitza resistance at the boundary between the ceramic and the helium, and inclusion of this resistance would reduce the temperature rise. Since heat must always travel more slowly than sound, heat which escapes into the liquid after the end of the application of the sound pulse cannot affect the nucleation process.

These considerations regarding the heat flow were the reason for using short sound pulses, *i.e.* 30 to 70 μs. Although it appears from the above discussion that the pulses are sufficiently short that heating effects are not of concern, it would certainly be of interest to perform a systematic study to confirm that this is correct.

2.1.5 Amplitude of the pressure swing

In the vicinity of the operating frequency both the thickness mode and high harmonics of the breathing mode are excited. Because of the overlap of the thickness mode with neighboring modes at nearby frequencies, it is not possible to calculate an exact value for the normal displacement ζ of the transducer surface. Moreover, since the low frequency breathing modes presumably have complicated displacement patterns, ζ may vary by a significant amount across the inner surface of the transducer. Despite these difficulties, it is still interesting to make a rough estimate of the magnitude of the pressure oscillation that would arise at the acoustic focus if the thickness mode was the only one excited. We have made a fit to the measured impedance in the frequency range around the thickness mode frequency using equation (2) with the parameters R, Q_0, and ω_0 treated as adjustable parameters. The fit gives $Q_0 = 121$, $R = 16\ \Omega$, $C = 81$ pF, and $\omega_0 = 1.014$ MHz. We can then calculate the displacement of the transducer surface for an applied drive voltage of amplitude $V_{\rm tran}$ and at the electrical resonance frequency ω_0 [15]

$$\zeta = \frac{V_{tran}}{8\pi\omega_0 R}\sqrt{\frac{RQ_0}{M\omega_0}}, \tag{3}$$

where M is the mass of the transducer ($M = 7.5$ g).

The voltage at the transducer is less than the voltage V applied at the top of the cryostat because of the 44 Ω resistance of the coaxial cable connecting the transducer. Allowing for this effect we finally obtain the result that the transducer displacement should be approximately 8 Å for an applied voltage of 1 V. This occurs only after the transducer has been driven for a time sufficient for the amplitude to reach an equilibrium value, *i.e.* after a time of order Q times the sound period. The characteristic time for the transducer amplitude to build up should in principle be affected by the impedance of the cable running to the driving amplifier and by the output impedance of the amplifier. However, we estimate that this time is approximately 5 μs, and hence is considerably less than the duration of the applied pulses.

Given this displacement, we can try to estimate the pressure swing ΔP at the focus. This is a very difficult problem because we are interested in pressure swings which are so large that the liquid at the focus nearly reaches the spinodal. As a consequence, the pressure swing must be significantly affected by the non-linearity of the sound propagation near to the focus. In addition, the magnitudes of the positive and negative pressure swings will differ. If the pressure swing is small, the positive and negative swings will be of the same size, and the amplitude of these swings will be linearly related to the magnitude $|\zeta|$ of the displacement at the transducer surface by [17]

$$\Delta P = |\zeta|\rho\omega^2 r_{tran}, \tag{4}$$

where ρ is the liquid density and r_{tran} is the radius of the hemispherical transducer. In liquid helium at low temperature and in the absence of an applied static pressure, $\rho = 0.145$ g cm^{-3}, and equation (4) with $r_{tran} = 0.8$ cm then predicts that to have a pressure oscillation at the focus with an amplitude of 1 bar it is necessary to have a displacement at the transducer surface of 22 Å. Thus to produce a pressure swing of 9 bars, *i.e.* a swing sufficient to reach to near to the spinodal, it should be necessary to apply 23 Volts to the transducer. This result is in excellent agreement with the results of the experiments that we present in Section 3, but this agreement is certainly fortuitous because of the effect of non-linearity.

2.2 Light scattering

To detect the light scattered by cavitation bubbles we used a photomultiplier tube (PMT) model R928 manufactured by Hamamatsu. Through the use of a small load resistor of 1000 Ω and a short connection to our digital oscilloscope *via* 50 Ω coaxial cables, we obtained an adequate sensitivity and a response time of less than 200 ns. In the absence of cavitation, the density oscillation at the focus scatters light through a small angle, typically 2×10^{-3} radians. We will refer to the signal arising from this scattered light as the acoustic signal. To measure the acoustic signal it was convenient to use a photomultiplier tube with a small diaphragm (0.5 mm) located at a small angle from the direction of the unscattered part of the laser beam and 50 cm away from the cell. A typical resonse is shown in the lower trace in Figure 3. This is the recording from a single sound pulse of duration 30 μs without any averaging. The acoustic signal begins at 33 μs which is the time it takes the sound to travel the 8 mm from the transducer surface to the focus at $P_{stat} = 0.8$ bar. Because of the short response time of the PMT it is possible to observe

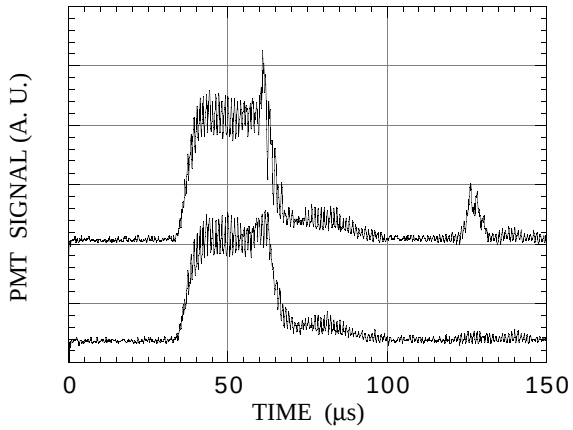

Fig. 3. This signal is the output voltage on the photomultiplier tube (PMT) as a function of time after the application of a driving voltage to the transducer. The lower trace shows the light which is scattered by the high amplitude sound wave at the acoustic focus (no cavitation in this case). This signal is maximized by setting the diaphragm in front of the PMT 2×10^{-3} radians away from the direct beam. The occurence of cavitation is visible on the upper trace which shows two new features. The feature at $t = 60$ μs results from the nucleation of a bubble at the end of the sound pulse. The bubble gives rise to additional light scattering. The feature at 126 μs is an echo of the cavitation event. It corresponds to sound which is reflected by the bubble back to the transducer and focussed again. The temperature in the cell was 0.5 K and the static pressure was 0.8 bar.

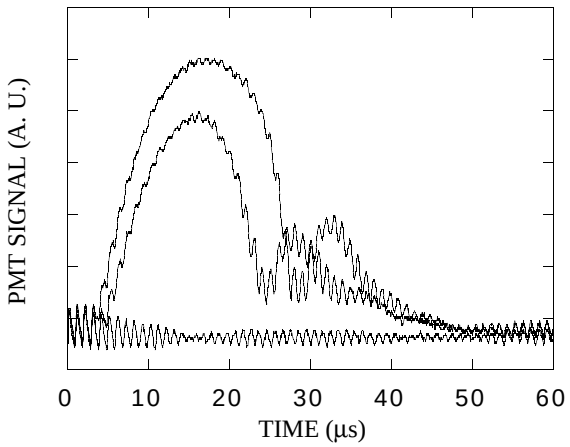

Fig. 4. Another recording of the light scattered by the sound wave (lower trace) and by two cavitation events (upper traces). Contrary to the previous figure, this recording is obtained with the PMT in the direct beam, so that the cavitation signal corresponds to all the light missing in the forward direction. Here, the temperature in the cell is 100 mK and the static pressure is 25 mbars only so that the life time of bubbles is much larger than in the previous case. The largest bubble nucleates one sound period earlier than the other one. In both cases, the collapse of the bubble gives birth to a second bubble with smaller size and energy.

the fluctuations in the intensity of the scattered light that take place at the frequency of the sound wave.

If cavitation occurs, the output of the PMT includes an extra sharp feature arising from light scattered by the nucleated bubble. An example of this is seen at around 60 μs in the upper trace in Figure 3. In this trace there is a second feature at about 126 μs. This feature arises from sound which is reflected from the nucleated bubble, returns to the transducer, and then is reflected back to the acoustic focus. Thus this feature is at a time of $2r_{tran}/c \approx$ 66 μs after the light scattering from the bubble itself.

The light scattered by a bubble is deflected at a larger angle than the light scattered from the density fluctuations produced by the sound. Consequently it is also possible to operate with a different detection scheme which emphasizes the signal from the bubble relative to the acoustic signal (Fig. 4). To use this method the diaphragm is put in the forward direction and its size chosen so that it captures nearly all of the light that is scattered by the sound oscillations as well as the unscattered part of the laser beam. Scattering from a bubble then gives a *reduction* in the light passing through the diaphragm. Since a bubble scatters light through an angle which is considerably larger than the angle subtended by the diaphragm, one can consider that in this geometry the bubble acts like an opaque disc with the same radius as the bubble r_{bubble}. At the optical focus which is located close to the acoustic focus, the laser beam has a Gaussian intensity profile proportional to $\exp(-2r^2/w^2)$ where r is the distance from the center of the beam and the beam waist is $w = 156 \pm 2$ μm. The signal from a bubble located at the center of the laser beam is thus $S(r_{bubble}) = S_0[1 - \exp(-2r_{bubble}^2/w^2)]$, where S_0 is the signal in the absence of bubble. Hence from a measurement of the reduction of the PMT signal the bubble size can be found [18], although noise prevents us from measuring radii less than 5 μm. This was adequate for the purpose of the present work, but could in the future be improved through the addition of a lens inside the cell with a smaller focal length so that w would be reduced. With the present large beam waist we have the advantage that the entire acoustic focus is illuminated so that all bubbles are sure to be detected.

The maximum radius r_{max} that is achieved by a bubble after nucleation decreases rapidly as the static pressure in the cell is increased. In addition, the lifetime τ_{bubble} of the bubbles becomes very short for large static pressures. If the time-dependence of the pressure at the location of the bubble is known the maximum size and the lifetime can be calculated from Rayleigh's theory [19]. Typically, the lifetime is 1 μs or less for P_{stat} greater than 1 bar.

3 Experimental results

The two traces in Figure 3 show the PMT response for two successive bursts of sound with the same amplitude and duration. Both measurements were made at $T = 0.5$ K and with $P_{stat} = 0.8$ bars with the diaphragm positioned so as to collect only the scattered light. As already described, for the lower trace there is no cavitation and the light is scattered by the acoustic wave only, whereas the upper

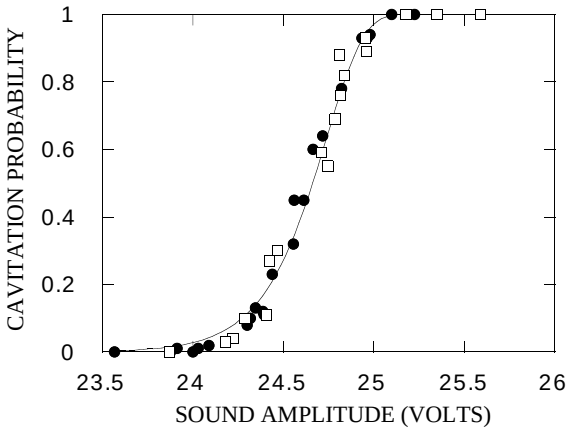

Fig. 5. Cavitation probability at 170 mK and 1 bar. The two sets of points correspond to data taken on two successive days with the same parameters. The solid line corresponds to equation (9). It shows that the process remains stochastic at low temperature.

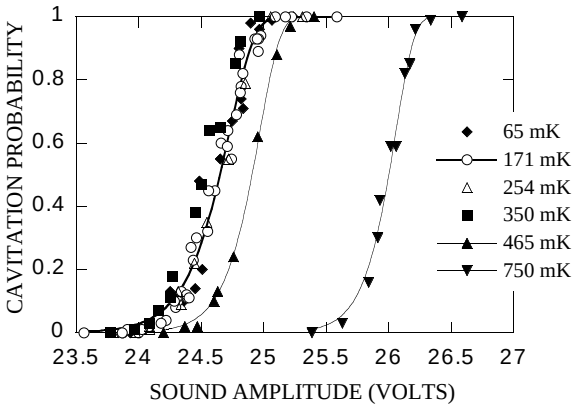

Fig. 6. Cavitation probability as a function of the voltage applied to the transducer for a series of different temperatures.

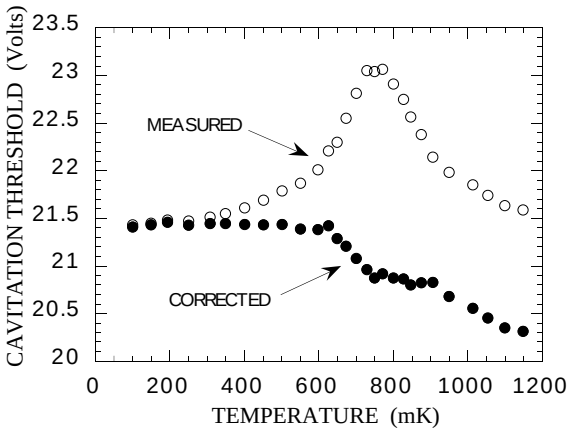

Fig. 7. The threshold voltage for cavitation V_c as a function of temperature. The raw data show a maximum at 750 mK which is due to the temperature variation of the sound attenuation. After correction for this effect, the cavitation threshold appears to be constant at low temperature ($T < 0.6$ K). Above 0.6 K, the threshold decreases monotonically with T as expected for a thermally activated nucleation.

trace shows the extra features that result from the nucleation of a bubble. When the applied voltage is just below the cavitation threshold, the response is the same for each pulse and has the form of the lower trace. At the threshold, some signals are like the lower trace, but some others have the form of the upper trace. As we increase the voltage V applied to the transducer, we observe a crossover from a situation where all signals are exactly like the lower trace to a situation where all signals are qualitatively like the upper trace, but actually not identical to it as discussed below.

By applying a number of sound pulses and counting the number of times the PMT response indicates nucleation, the probability Σ of nucleation can be determined. By Σ we mean the probability that at least one bubble appears, or equivalently one minus the probability of having no cavitation at all.

We first measured the cavitation probability $\Sigma(V,T)$ as a function of applied voltage and temperature. A typical curve is shown in Figure 5. It corresponds to a static pressure P_{stat} of 0.8 bar and a temperature of 170 mK. The two sets of points correspond to measurements taken on consecutive days, and indicate the stability of our experiment.

Figure 6 shows a set of similar curves corresponding to successive temperatures from 65 mK to 750 mK. From these data it is clear that the cavitation probability depends on temperature only above about 400 mK.

Typically, the transition from no cavitation to cavitation with a probability close to one occurs over a voltage range of about 4%. We define the cavitation threshold as the voltage V_c at which the cavitation probability is 0.5. In Figure 7 we show V_c as a function of temperature in the range 65 to 1200 mK. The measurements on this figure correspond to the saturated vapor pressure, *i.e.* $P_{stat} \approx 0$.

It can be seen that V_c shows a maximum at 750 mK. We believe that this maximum is mainly due to the attenuation of sound. An increase in sound attenuation has the consequence that a larger voltage is needed to give the same pressure swing at the acoustic focus. It is well known [3] that the sound attenuation has a strong peak at the temperature where the roton-phonon scattering time equals the sound period. The attenuation has been measured by Waters *et al.* [20] at a series of frequencies down to 1.69 MHz. We have extrapolated their results to estimate the attenuation at 1 MHz. To perform the extrapolation plots of $\log(\alpha)$ *versus* $\log(\omega)$, where α is the attenuation and ω is the frequency, were made at each temperature. These plots were extrapolated linearly to find the attenuation at 1 MHz. In order to check this extrapolation, we made an independent measurement of the attenuation through a study of the magnitude of the acoustic signal. The acoustic signal can be divided into two contributions, one part which fluctuates at the frequency of the sound wave and a second part S_{dc}, the "dc component", which varies slowly with time. We first investigated how the dc part S_{dc} varied with the amplitude of the transducer

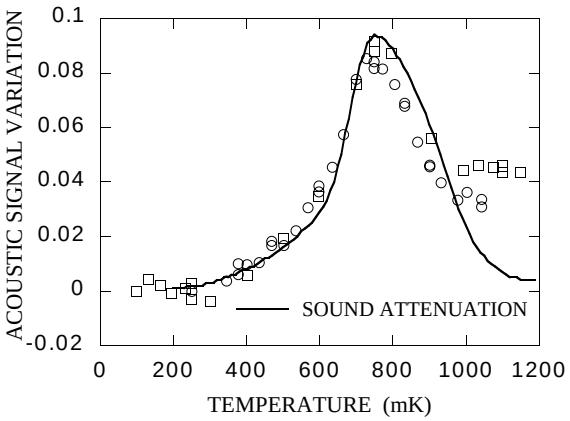

Fig. 8. The relative change in voltage which is necessary for a constant sound amplitude at the focus. A comparison with the known attenuation of sound shows that, up to 900 mK, the observed temperature variation of the sound amplitude is mainly due to this attenuation. Above 900 mK, other effects can play a role, since the sound velocity itself starts varying with T. We used our experimental measurement to correct the data in Figure 7.

driving voltage V. We found that S_{dc} was proportional to V^2. This is expected if the light scattering is proportional to the square of the local density oscillations which are themselves approximately linear in V. We then measured S_{dc} as a function of T for constant drive voltage applied to the transducer. The variation in S_{dc} with temperature arises from the attenuation of the sound that travels from the transducer to the focus, and hence the measurement of $S_{dc}(T)$ can be used to find the ultrasonic attenuation.

The results for the attenuation are shown in Figure 8, and up to 0.9 K are in very good agreement with the extrapolation of the results of Waters *et al.* [20]. Above this temperature, the two methods do not agree. We do not know the definite explanation for this. It is possible that the method we used to extrapolate the Waters data is inadequate. It is also likely that above 0.9 K the temperature variation of the density is such that it affects the pressure amplitude at the focus. Indeed, equation (4) shows that it is directly proportional to the density; furthermore, we believe that diffraction from the ceramic edges produce an interference pattern which also depends on the sound velocity, consequently on temperature. We decided to use our own measurement of the sound amplitude at the focus (more precisely the amplitude of the dc part of the acoustic signal) to correct the cavitation data. The result of applying this correction to the cavitation data is included in Figure 7. We do not think that the slight wiggles on the corrected data near 0.8 K are significant. Near this temperature where dissipation is important it should be necessary to include some heating of the focal region in the correction.

4 Comparison with quantum tunneling theory

After correction, the cavitation voltage is found to be independent of temperature up to 0.6 K (Fig. 7). Above this temperature the voltage decreases as T increases, as expected for thermally activated nucleation. It is natural to interpret this result as a crossover from quantum cavitation proceeding *via* tunneling below 0.6 K to thermally-activated classical cavitation. Here we discuss in some detail the extent to which different aspects of the data are consistent with this interpretation.

4.1 Stochastic nature of the nucleation

The measurements clearly indicate that over the entire temperature range the nucleation process is stochastic when the voltage lies in a range around the cavitation threshold. This result, combined with the observation that the threshold voltage is independent of temperature, is a strong evidence for quantum nucleation. If at 100 mK, for example, the nucleation was occuring as a result of the pressure swing reaching the spinodal rather than by quantum tunneling through a barrier at a pressure close to the spinodal, then the nucleation would not be stochastic. A plot of Σ as a function of V should then show a jump from 0 to 1 at some voltage.

One can ask how the nucleation could be stochastic at the lowest temperatures without quantum tunneling being the mechanism. We have considered the possibility that noise or drift in the electric signal used to drive the transducer could give stochastic behavior. If there is noise on the voltage applied to the transducer, then for some pulses the pressure will reach the spinodal while for others the pressure swing will not be as large. This would then replace the step in Σ with a smooth increase over a voltage range determined by the magnitude of the noise. However, we can rule out this possibility. The voltage applied to the transducer fluctuates by only $\sim 0.1\%$ even over a few hours, and this is much less than the width of the transition region in $\Sigma(V)$. We also measured the fluctuations in the frequency of the applied pulse, these fluctuations were found to have a magnitude of around $\pm 0.01\%$.

We investigated whether there was a correlation between the probability of cavitation and these small fluctuations in the applied voltage and frequency. There was no sign of any significant correlation.

4.2 Shape of the plot of Σ versus V

The plots of Σ as a function of the transducer voltage at all temperatures have a characteristic shape (Fig. 6). The probability curve has a rounded foot and a sharper head. The nucleation rate for quantum tunneling per unit time and per unit volume of liquid is

$$\Gamma = \Gamma_0 \exp(-B/\hbar) \tag{5}$$

where Γ_0 is the attempt rate and B is the action associated with the motion though the tunneling barrier. Hence, when measurements are made for a time τ_{exp} on a volume of liquid V_{exp} the probability that nucleation will occur is

$$\Sigma = 1 - \exp\left[-\Gamma_0 V_{exp}\tau_{exp}\exp(-B/\hbar)\right]. \quad (6)$$

Both B and Γ_0 will vary with pressure but, of course, the variation of B makes the main contribution to the variation of Σ with P. We define the critical action B_c as the value of B which corresponds to a nucleation probability of 0.5. Then

$$B_c = \ln\left[\frac{\Gamma_0 V_{exp}\tau_{exp}}{\ln 2}\right]. \quad (7)$$

We then expand B to first order in the pressure relative to the pressure P_c that corresponds to B_c to obtain

$$\Sigma = 1 - \exp\left\{-\ln 2\exp\left[-\left(\frac{d\ln B}{d\ln P}\right)_{P=P_c}\frac{B_c(P-P_c)}{\hbar P_c}\right]\right\}. \quad (8)$$

If we further assume that over the range in which Σ goes from 0 to 1 the derivative of the pressure with respect to applied voltage is linear, we have

$$\Sigma = 1 - \exp\left\{-\ln 2\exp\left[-\left(\frac{d\ln B}{d\ln P}\right)_{P=P_c}\times\left(\frac{d\ln P}{d\ln V}\right)_{P=P_c}\frac{B_c(V-V_c)}{\hbar V_c}\right]\right\}. \quad (9)$$

In Figure 5 the solid curve is a fit to the experimental data based on equation (9) with the quantity

$$\xi \equiv B_c(d\ln B/d\ln P)_{P=P_c}(d\ln P/d\ln V)_{P=P_c}$$

treated as an adjustable parameter. One can see that this fit reproduces the shape of the $\Sigma(V)$ curve very well.

It is important to note that this characteristic shape of the curve of Σ as a function of V does not by itself constitute evidence that the nucleation is the result of quantum tunneling. The same shape curve would result from thermally-activated nucleation [10]. However, the fact that the shape is correctly predicted by equation (9) does give further support to the argument that the results are not affected by noise or drift in the electrical signal used to drive the transducer. If noise were important one would not expect the $\Sigma - V$ curve to have the asymmetry that is observed.

4.3 Action, cavitation pressure and width of the transition region

First we estimate the action B_c from equation (7). This needs values of Γ_0, V_{exp} and τ_{exp}. In reference [8] an order of magnitude estimate of Γ_0 has given $\Gamma_0 = 2\times 10^{31}$ cm^{-3} s^{-1}.

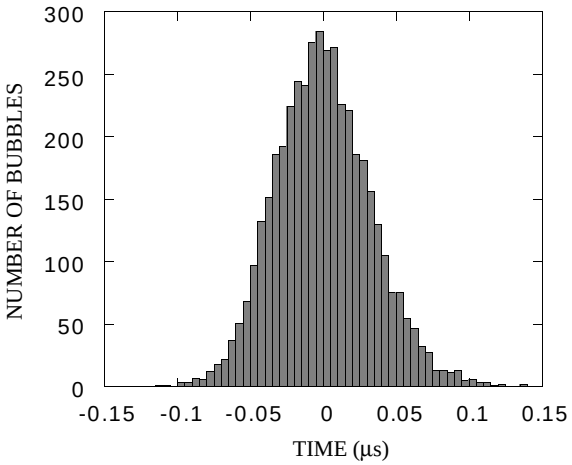

Fig. 9. Histogram of the birth dates of bubbles. Cavitation occurs near the minimum in the last negative pressure swing of the sound pulse. Here, a short pulse of 44 μs was used. The width of this distribution is used to measure the experimental time (83 ns).

In a previous article [10], we have estimated V_{exp} and τ_{exp} on the assumption that non-linear effects do not significantly modify the sinusoidal shape of the wave. We made this estimate in the context of an analysis of thermally-activated nucleation. If we applied the same approach in the present context we would obtain:

$$V_{exp} = \lambda^3\left(\frac{3}{2\pi D}\right)^{3/2}, \quad \tau_{exp} = \tau\left(\frac{1}{2\pi D}\right)^{1/2} \quad (10)$$

per negative pressure swing, where λ and τ are the acoustic wavelength and period, respectively, and

$$D = (B_c/\hbar)(d\ln B/d\ln P).$$

Combining equations (7) and (10) we would obtain the condition

$$B_c = \ln\left[\frac{2\times 10^{31}\ 3^{3/2}\ \lambda^3\ \tau}{4\pi^2\ \ln 2}\right] - 2\ln\left[\frac{B_c}{\hbar}\left|\frac{d\ln B}{d\ln P}\right|_c\right]. \quad (11)$$

The variation of B with pressure has been calculated by Maris [8], and some numerical values are listed in Table 1. From these results and equation (11) we would obtain the values $B_c = 32\hbar$, $d\ln B/d\ln P\big|_c = -22.6$ and $V_{exp}\tau_{exp} = 3.1\times 10^{-18}$ cm^{3}s. This would correspond to a pressure $P_c = -9.27$ bars, *i.e.* 0.25 bars from the spinodal which is predicted to occur at a pressure -9.52 bars.

However, numerical simulations [21] have shown that non-linear effects broaden the pressure minima and sharpen the maxima of the wave, both in space and in time. Thus, the product $V_{exp}\tau_{exp}$ should be somewhat larger than estimated above. To investigate this we recorded the times at which nucleation took place. Typical results are shown in Figure 9. We find that for each

negative pressure swing the nucleation occurs over a time range of about 83 ns, significantly more than 15 ns, the value predicted by equation (10). We have then calculated the experimental volume by using the equation of propagation of sound

$$\Delta P - (1/c^2(P_{min})(\partial^2 P/\partial t^2) = 0$$

near the minimum pressure P_{min} (c is the sound velocity). We obtained

$$V_{exp} = \left(c(P_{min})\sqrt{3}\tau_{exp}\right)^3. \quad (12)$$

We finally used the equation of state by Maris [8] to calculate the sound velocity:

$$c = A(P - P_{spin})^{1/3}. \quad (13)$$

In this equation, P_{spin} is the spinodal pressure and the constant $A = 112$ CGS units. We finally obtained

$$V_{exp}\tau_{exp} = 1.0 \times 10^{-16}\ \mathrm{cm^3 s} \approx \left(\frac{\lambda}{22}\right)^3\left(\frac{\tau}{12}\right). \quad (14)$$

This means about ten microns cubed and a time of 0.1 μs, *i.e.* a volume and a time which are small but macroscopic. In such an experiment, to approach the spinodal more closely would require work at much higher frequency. It is also interesting to note here that the distribution in nucleation times leads to a distribution in the final bubble sizes, and consequently also in the amplitude of the cavitation signals. Indeed, the sooner bubbles nucleate, the more time they have to acquire kinetic energy from the negative swing of the sound oscillation. This is why the acoustic signal is quantitatively reproducible from one pulse to the next, while cavitation signals are only qualitatively similar to one another (see Fig. 4). If we then suppose that cavitation occurs during only one swing, we obtain the value of the action B_c from equation (7):

$$B_c = 35.6\ \hbar. \quad (15)$$

We then estimate the value of the cavitation pressure and the energy barrier from Table 1:

$$P_c = -9.23\ \mathrm{bars}, \quad E = 10.5\ \mathrm{K}. \quad (16)$$

At $P = -9.23$ bars, the sound velocity is $c = 75$ m/s. Our final values differ only slightly from our first estimate.

Finally, it is possible to analyze the width of the transition region, which is related to

$$\xi \equiv B_c(d\ln B/d\ln P)_{P=P_c}(d\ln P/d\ln V)_{P=P_c}.$$

From table 1, we also deduce

$$\left(\frac{d\ln B}{d\ln P}\right)_{P=P_c} = -20.3 \quad (17)$$

and we can use the experimentally determined value $\xi = 124\hbar$ to obtain

$$\left(\frac{d\ln P}{d\ln V}\right)_{P=Pc} = 0.17. \quad (18)$$

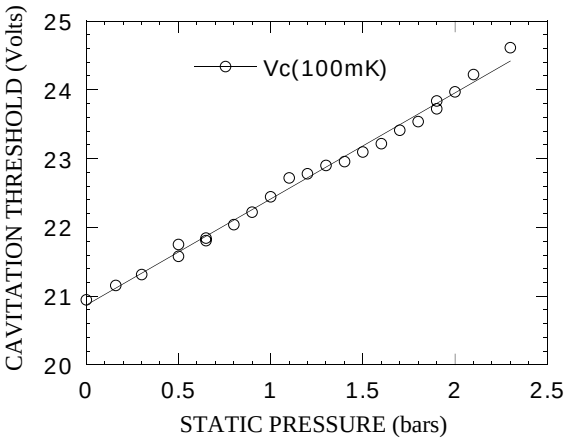

Fig. 10. The variation of the cavitation threshold as a function of the static pressure in the cell.

For very small sound amplitudes the pressure swing at the focus must be linear in the driving voltage and so $d\ln P/d\ln V = 1$. As expected, numerical simulations indicate [21,22] that $d\ln P/d\ln V$ decreases as the pressure swing increases which is consistent with the above result. Thus 0.17 is a reasonable value. However, we have not yet succeeded in making a quantitative calculation of $d\ln P/d\ln V$ in the vicinity of the spinodal.

4.4 Variation with static pressure

We have tried to confirm the above estimate of the cavitation pressure by studying the variation of the cavitation voltage V_c with the static pressure P_{stat} or static density ρ_{stat}. As shown in Figure 10, our results are more precise, also restricted to a smaller pressure domain than those presented in our previous article [10]. Above a static pressure of about 2.5 bars, the lifetime of bubbles is too short and cavitation can be seen only if the voltage is large enough to nucleate big bubbles. As a consequence, small events are not detected and the apparent cavitation threshold increased. This is the explanation for the slight upward curvature which was observed by Pettersen *et al.* [10] on their plot of V_c *versus* P_{stat} at small P_{stat}. We believe that this upward curvature was an artefact, and we thus restricted our present study to the small pressure interval ($0 < P_{stat} < 2.5$ bars) where the bubble lifetime is significantly larger than the response time of our detection system. If we neglected non linear effects, we could extrapolate down to the pressure where V_c vanishes and obtain the cavitation density and pressure. We tried such a linear extrapolation, but we actually plotted the quantity ρV_c as a function of P_{stat} because the amplitude of the pressure oscillation is proportionnal to the static density (Eq. (4)). We obtained $P_c = -11.5$ bars. This is the right order of magnitude but more negative than the spinodal pressure. We found this result independent of temperature below 0.4 K. We also believe that non linear effects are likely to decrease the magnitude of the negative pressure swing with respect to the prediction from the linear

Table 1. Results of the calculation by Maris [8] of the negative pressure P, the energy barrier E and the action B for the nucleation of bubbles in helium-4, and the sound velocity c as a function of the density ρ near the spinodal density ρ_{sp}= 0.09482 g cm^{-3}.

ρ (g cm^{-3})	$\rho - \rho_{sp}$ (g cm^{-3})	P (bars)	E (K)	$B/\hbar$	$d\ln B/d\ln P$	c (m s^{-1})
0.1088	0.01398	−9.32	8.2	28.8	−25.4	66
0.1092	0.01438	−9.30	8.7	30.2	−24.1	68
0.1096	0.01478	−9.28	9.2	31.7	−23.0	70
0.1100	0.01518	−9.26	9.7	33.2	−21.8	72
0.1104	0.01558	−9.24	10.2	34.9	−20.7	74
0.1108	0.01598	−9.22	10.8	36.6	−19.7	76
0.1112	0.01638	−9.19	11.4	38.5	−18.7	78
0.1116	0.01678	−9.17	12.0	40.4	−17.8	79
0.1120	0.01718	−9.14	12.6	42.4	−16.9	81
0.1124	0.01758	−9.12	13.2	44.6	−16.0	83
0.1128	0.01798	−9.09	13.9	46.9	−15.2	85

law (Eq. (4)). We hope to check this and compare with the estimated value −9.23 bars when we succeed in including non-linear effects in the numerical calculation of ΔP *versus* driving amplitude and static pressure. If this led to an accurate enough estimate of P_c, we could also discriminate between the homogeneous nucleation which is assumed here and a nucleation mediated by vortex lines which has also been suggested [22,23]. The presence of vortex lines in large enough density could reduce the cavitation threshold by one or two bars. In the absence of a theory of quantum nucleation of bubbles on vortex cores, we cannot say if it is compatible with our results, but this possibility is not excluded.

4.5 Crossover temperature

The measurements indicate that the voltage required to cause nucleation becomes independent of temperature below 0.6 K. At first sight this can be taken to indicate that the crossover temperature T^* to quantum nucleation is 0.6 K. This is significantly higher than 0.2 K, the currently accepted theoretical prediction [8,9]. We believe that there is a simple explanation for this apparent discrepancy. In a first approximation the acoustic wave is adiabatic, and consequently the temperature oscillates at the focus, as well as the pressure. At temperatures below 0.7 K, phonons make the dominant contribution to the entropy [3], and the entropy per unit mass is

$$S \approx S_{ph} = \frac{2\pi^2 k_B^4 T^3}{45\rho\hbar^3 c^3} \cdot \qquad (19)$$

Hence in an isentropic process the temperature is proportional to the sound velocity c. At $P = -9.23$ bars, we have seen that the sound velocity is 75 m s^{-1}, a factor 3 lower than at zero pressure ($c = 238$ m s^{-1}). As a consequence, the local, instantaneous temperature T should be lowered at the focus by the same factor 3 with respect to the static temperature T_{stat} of the cell. Thus the measured T_{stat} at which the crossover to quantum nucleation takes place is in fact consistent with the theoretical prediction.

5 Conclusions

We have studied the nucleation of bubbles in helium at negative pressures in the temperature range down to 65 mK. The results are consistent with the idea that below 0.6 K the nucleation is the result of quantum tunneling through the nucleation barrier. We have discussed the evidence for this which is provided by the experiment and considered a number of possible artefacts. Our interpretation led us to the conclusion that, in our experiment, the quantum nucleation of bubbles takes place at the negative pressure $P_c = -9.23$ bars, *i.e.* 0.29 bar above the spinodal pressure. Of course a direct measurement of the instantaneous pressure of the focussed sound wave would bring an important check of this conclusion. Such a new measurement would also allow us to consider the possibility that cavitation is assisted by the presence of vortices. Our measurements are not yet accurate enough to rule out such a possibility. Finally, measurements of cavitation at low temperature in liquid helium 3 are in progress. We expect that they will provide an interesting comparison with helium 4, since the spinodal pressure of liquid helium 3 is predicted to be around − 3 bars [8,9].

This work was supported in part by the US National Science Foundation through grant no. DMR 91-20982 and by the CNRS-NSF collaboration program through grant INT 93-14295.

References

1. E. Roedder, Science **155**, 1413 (1967).
2. D.H. Trevena, *Cavitation and tension in liquids* (Hilger, Bristol, 1987).

3. J. Wilks, *The Properties of Liquid and Solid Helium* (Clarendon Press, Oxford 1967)
4. H.J. Maris , J. Low Temp. Phys. **94**, 125 (1994).
5. F. Dalfovo, A. Lastri, L. Pricaupenko, S. Stringari, J. Treiner, Phys. Rev. B **52**, 1193 (1995).
6. J. Boronat, J. Casulleras, J. Navarro, Phys. Rev. B **50**, 3427 (1994).
7. I.M. Lifshitz, Yu. Kagan, Zh. Eksp. Teor. Fiz. **62**, 385 (1972) (Sov. Phys. JETP **35**, 206 (1972)).
8. H.J. Maris, J. Low Temp. Phys. **98**, 403 (1995).
9. M. Guilleumas, M. Pi, M. Barranco, J. Navarro, M.A. Solis, Phys. Rev. B **47**, 9116 (1993); M. Guilleumas, M. Barranco, D.M. Jezek, R.J. Lombard, M. Pi, Proc. LT21, Czech. J. Phys. **46**, Suppl. S1, 389 (1996) and Phys. Rev. B **54**, 16135 (1996); D.M. Jezek, M. Guilleumas, M. Pi, M. Barranco, Europhys. Lett., **38**, 601 (1997).
10. M.S. Pettersen, S. Balibar, H.J. Maris, Phys Rev. B **49**, 12062 (1994).
11. E. Rolley, C. Guthmann, E. Chevalier, S. Balibar, J. Low Temp. Phys. **99**, 851 (1995).
12. J.A. Nissen, E. Bodegom, L.C. Brodie, J.S. Semura, Phys. Rev. B **40**, 6617 (1989).
13. Manufactured by Quartz et Silice, France, type P7-62
14. H.T. O'Neil, J. Acoust. Soc. Amer. **21**, 516 (1949); C.W. Smith, R.T. Beyer, J. Acoust. Soc. Amer. **46**, 806 (1969).
15. D.A. Berlincourt, D.R. Curran, H. Jaffe, *Physical Acoustics*, Vol. **1A**, edited by W.P. Mason (Academic Press, New York and London, 1964), p. 229.
16. We use the values of the specific heat and the thermal conductivity for $PbZrO_3$ as measured by W.N. Lawless, Phys. Rev. B **30**, 6555 (1984). The thermal diffusivity of a ceramic depends on the grain size, which for our PZT transducer was about 3 μm. We note that a diffusivity of 4 $cm^2\,s^{-1}$ at 3 K is within the typical range for other ceramics with a grain size of 3 μm. See, *Experimental Techniques in Condensed Matter Physics at Low Temperatures*, edited by R.C. Richardson, E.N. Smith (Addison and Wesley, New York, 1988), p. 118.
17. L.D. Landau, E.M. Lifshitz, *Course of Theoretical Physics Vol. 6: Fluid Mechanics* (Pergamon Press, Oxford).
18. P. Roche, H. Lambaré, E. Rolley, D. Lacoste, S. Balibar, C. Guthmann, H.J. Maris, Proc. LT21, Czech. J. Phys. **46**, Suppl. S1, 381 (1996).
19. Lord Rayleigh, Philos. Mag. **34**, 94 (1917).
20. G.A. Waters, D. Watmough, J. Wilks, Phys. Lett. **26A**, 12 (1967). Unpublished data at 1.69, 3.00 and 4.65 MHz were kindly communicated to us by Dr Waters.
21. H. Lambaré, C. Appert, to be published.
22. Q. Xiong, H.J. Maris, J. Low Temp. Phys. **82**, 105 (1994).
23. F. Dalfovo, Phys. Rev. B **46**, 5482 (1992); F. Dalfovo, G. Renversez, J. Treiner, J. Low Temp. Phys. **89**, 425 (1992).